ChemComm

Accepted Manuscript

This article can be cited before page numbers have been issued, to do this please use: S. Lv, L. Han, J. Xiao, L. Zhu, J. Shi, H. Wei, Y. Xu, J. Dong, X. Xu, D. Li, S. Wang, Y. Luo, Q. Meng and X. Li, *Chem. Commun.*, 2014, DOI: 10.1039/C4CC02211D.

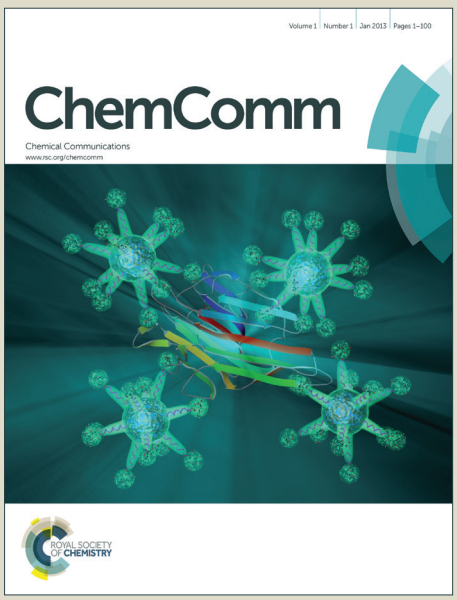

ROYAL SOCIETY OF CHEMISTRY

www.rsc.org/chemcomm

View Article Online
DOI: 10.1039/C4CC02211D

Journal Name

RSCPublishing

COMMUNICATION

Mesoscopic $TiO_2/CH_3NH_3PbI_3$ perovskite solar cells with new hole-transporting materials containing butadiene derivatives

Cite this: DOI: 10.1039/x0xx00000x

Received 00th January 2012,
Accepted 00th January 2012

DOI: 10.1039/x0xx00000x

www.rsc.org/

Songtao Lv,[a] Liying Han,[b] Junyan Xiao,[a] Lifeng Zhu,[a] Jiangjian Shi,[a] Huiyun Wei,[a] Yuzhuan Xu,[a] Juan Dong,[a] Xin Xu,[a] Dongmei Li,*[a] Shirong Wang,[b] Yanhong Luo,[a] Qingbo Meng*[a] and Xianggao Li*[b]

Two new triphenylamine-based hole-transporting materials (HTMs) containing butadiene derivatives are employed in $CH_3NH_3PbI_3$ perovskite solar cells. Up to 11.63% of power conversion efficiency (PCE) has been achieved. Advantages of easy synthesis, low cost and relatively good cell performance exhibit a possibility for commercial application in the future.

Organolead halide perovskites have attracted lots of interests due to their outstanding advantages of direct band gap, large absorption coefficient and high carrier mobility.[1,2] In 2009, T. Miyasaka pioneered organolead halide perovskites as sensitizers in liquid-type sensitized solar cells with power conversion efficiencies (PCEs) of 3.13% for $CH_3NH_3PbBr_3$ and 3.81% for $CH_3NH_3PbI_3$, which was further improved to 6.5% by N.-G. Park.[3,4] Over the last two years, solid-state organolead halide perovskite thin film solar cells developed rapidly, and unexpected breakthrough has been achieved.[5,6] It is expected that the perovskite solar cell is comparable to conventional thin film solar cells (Cu(In,Ga)Se_2, CdTe). Currently, perovskite solar cells with and without hole-transporting materials (HTMs) have been developing. The perovskite solar cells without HTMs exhibited a PCE over 10%,[7] whereas the corresponding devices with HTMs can exhibit much higher efficiencies, over 16% so far.[8] The use of HTMs is often perceived to impart some advantages to the cells, mainly facilitating the hole transport to metal anode and blocking the electron transfer from perovskites to metal anode as well.

Different HTMs have already been demonstrated to work well in perovskite solar cells. First, a few polymer HTMs were successfully applied in this kind of solar cells, such as poly(3-hexylthiophene) (P3HT), poly-triarylamine (PTAA), poly[2,1,3-benzothiadiazole-4,7-diyl[4,4-bis(2-ethylhexyl)-4H-cyclopenta[2,1-b:3,4-b']dithiophene-2,6-diyl]] (PCPDTBT) and so on.[9-12] Typically, the perovskite solar cells with PTAA exhibited 12% of PCE.[9] Moreover, low molecular weight amorphous HTMs are also good candidates due to their easy purification and good film-forming property simply processed by coating technique. Based on state of the art *spiro*-OMeTAD (2,2',7,7'-tetrakis[N,N-di-*p*-methoxyphenylamine]-9,9'-spirobi fluorene) as the HTM, M. Grätzel,[13] H. J. Snaith[14] and T. L. Kelly[15] obtained over 15% of PCEs by using different mesoporous scaffolds or planar heterojunction structures, respectively. And $CH_3NH_3PbI_3$ perovskite solar cells with pyrene arylamine derivatives presented 12.4% of PCE.[16] Besides organic HTMs, inorganic hole conductor like CuI with higher conductivity in the perovskite solar cells was also explored, achieving 6% of PCE.[17] However, current HTMs for this kind of solar cells suffer from high cost or unsatisfactory cell performance, both of which are disadvantageous for future commercialization. Therefore, it is urgent to develop new HTMs for stable, highly efficient and cost-effective perovskite solar cells.

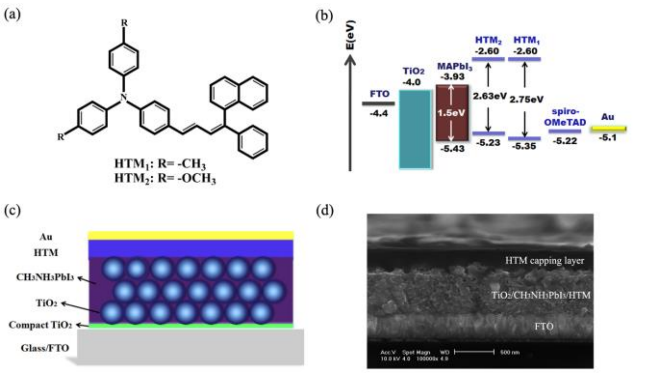

Fig. 1 (a) Molecular structures of HTMs; (b) Energy level diagram of perovskite solar cells with three HTM materials; (c) Device configuration of the perovskite solar cells; (d) Cross-sectional SEM image of FTO/TiO_2/$CH_3NH_3PbI_3$/HTM_2 film (120 mg mL^{-1} HTM_2 chlorobenzene solution).

Suitable HTMs for perovskite solar cells should primarily meet following requirements: (1) good hole mobility; (2) compatible HOMO energy level relative to organolead halide perovskite and (3) low cost for commercialization. The triphenylamine entities with butadiene derivatives are known as high hole mobility and good film-forming property, which were applied in organic photo conductors (OPCs).[18] In this respect, two new triphenylamine-based hole conductors containing butadiene derivatives have been used in $CH_3NH_3PbI_3$ perovskite solar cells for the first time, which are 4-(4-phenyl-4-α-naphthylbutadienyl)-N,N-di(4-tolyl)-phenylamine (denoted as

HTM_1), and 4-(4-phenyl-4-α-naphthylbutadienyl)-N,N-di(4-methoxyphenyl)-phenylamine (denoted as HTM_2), respectively, as shown in Fig. 1(a). Under AM1.5 irradiation (100 mW cm^{-2}), the PECs of 11.63% for HTM_2 and 11.34% for HTM_1 have been achieved, in comparison with the PCE for the cell with *spiro*-OMeTAD (12.08%). Our preliminary results reveal that both HTM_1 and HTM_2 are promising alternatives to *spiro*-OMeTAD. And they are quite cheap for potential commercialization.

HTM_1 and HTM_2 were synthesized from Wittig-Horner reaction, which detailed procedures for the syntheses and characterization can be found in our previous work.[18] Their maximum absorption bands are located in the visible region, which are 451 nm for HTM_1 and 471 nm for HTM_2, respectively. At room temperature, their hole transporting mobilities are evaluated by time-of-flight (TOF) transient hole-current measurement, which are 2.98×10^{-3} for HTM_1 and 1.27×10^{-3} $cm^2 \cdot V^{-1} \cdot S^{-1}$ for HTM_2, respectively. The energy levels of HTM_1 and HTM_2 are determined by ultraviolet photoelectron spectroscopy (UPS) and cyclic voltammetry (CV) measurements, as shown in Fig. 1(b). It is thus deduced that different *p*-position substituents (electron-donating ability -OCH_3>-CH_3) on phenyl rings of the triphenylamine part do not strongly influence their energy levels since triphenylamine and butadiene derivatives form a large π-conjugated system. Moreover, both HTMs have suitable HOMO level in comparison to the valence band of $CH_3NH_3PbI_3$ (-5.43 eV), suggesting good HTMs for $CH_3NH_3PbI_3$ perovskite solar cells.

For fabricating the device (see Fig. 1(c)), 50 nm-thickness TiO_2 compact layer and 400 nm-thickness mesoporous TiO_2 anatase layer were deposited on FTO glass in sequence according to the literature.[5] $CH_3NH_3PbI_3$ was subsequently deposited on the mesoporous TiO_2 film by using a sequential method as reported.[13] HTMs with proper concentrations were spin-coated on the mesoporous $TiO_2/CH_3NH_3PbI_3$ film at 3000 rpm for 20s, and an 80 nm-thickness Au layer was finally deposited on the top of the HTM layer by thermal evaporation. For comparison, the device with *spiro*-OMeTAD was also fabricated by the same condition. Fig. 1(d) shows the cross-sectional scanning electron microscopy (SEM, FEI, XL30 S-FEG) image of $FTO/TiO_2/CH_3NH_3PbI_3/HTM_2$ film with 120 mg mL^{-1} HTM solution. We can see that $CH_3NH_3PbI_3$ is evenly distributed in TiO_2 mesoscopic pores. And 271 nm-thickness HTM_2 capping layer is observed whereas no obvious capping layer when using 20 mg mL^{-1} HTM_2.

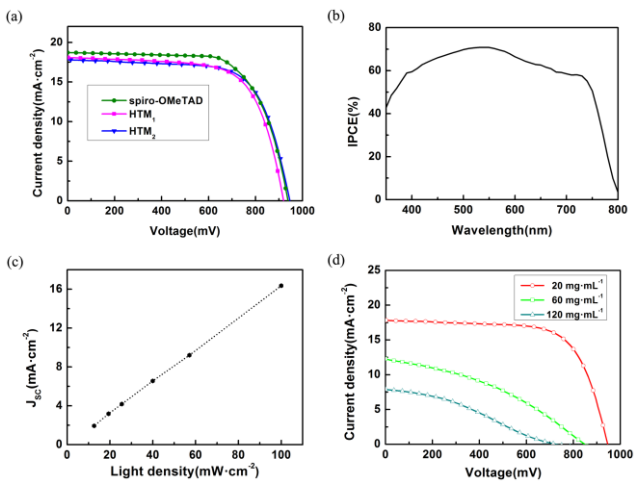

Fig. 2 (a) *J-V* curves for the perovskite solar cells fabricated with HTM_1, HTM_2 and *spiro*-OMeTAD; (b) IPCE spectrum of the cell with HTM_2. The concentration of the HTMs: 20 mg mL^{-1} solution in chlorobenzene; (c) Plot of the J_{sc} of $CH_3NH_3PbI_3$ perovskite solar cells with HTM_2 *vs.* light densities; (d) *J-V* curves for the perovskite solar cells with different HTM_2 concentration.

Fig. 2(a) shows photocurrent density-photovoltage (*J-V*) curves of three cells with different HTMs. All of the three HTM films were obtained from 20 mg mL^{-1} solution in chlorobenzene. We can see that, when new HTMs are introduced into the device, the PCEs are 11.34% for HTM_1 with short-circuit photocurrent density (J_{sc}) of 18.1 mA cm^{-2}, open-circuit photovoltage (V_{oc}) of 921 mV and fill factor (*FF*) of 0.68 and 11.63% for HTM_2 with J_{sc} of 17.9 mA cm^{-2}, V_{oc} of 942 mV and *FF* of 0.69, respectively. These are comparative to that of *spiro*-OMeTAD-based perovskite solar cells under the same fabrication method, which photovoltaic parameters are J_{sc} of 18.7 mA cm^{-2}, V_{oc} of 936 mV, and *FF* of 0.69, yielding 12.08% of PCE, in agreement with those reported by S. I. Seok.[19] The V_{oc} of the devices with HTM_2 and *spiro*-OMeTAD are close, in agreement with their similar HOMO levels since the theoretical V_{oc} is determined by the difference in the quasi-Fermi levels of the electrons in the TiO_2 and the holes in the HTM. However, the V_{oc} of the HTM_1-based device is slightly lower, which is abnormal since its HOMO level is relatively lower, see Table. S1. The origin of this phenomenon is still not fully understood so far, however, the dependence of the V_{oc} on the HTMs is also influenced by charge recombination kinetics.[16] The monochromatic incident photon-to-electron conversion efficiency (IPCE) spectrum of the cell with HTM_2 is presented in Fig. 2(b).[20] An integral photocurrent from the overlap of the IPCE spectrum is 15.8 mA cm^{-2}, basically in agreement with the experimentally obtained J_{sc}. Besides, the above result further confirms that the two substituents (-CH_3 and -OCH_3) do not strongly influence their HOMO levels and the cell performance. So, we will take HTM_2 as an example to further investigate the properties of the cell in the following discussion.

The dependence of J_{sc} of the device with HTM_2 on light densities is also investigated. As shown in Fig. 2(c), the J_{sc} is linearly proportional to light density, indicating that the charge collection efficiency in the device is independent with light intensities. According to previous investigation, it is suggested that no space-charge limit exists in the $TiO_2/CH_3NH_3PbI_3/HTM_2$ junction due to small difference in the mobility between electrons and holes.[5,21]

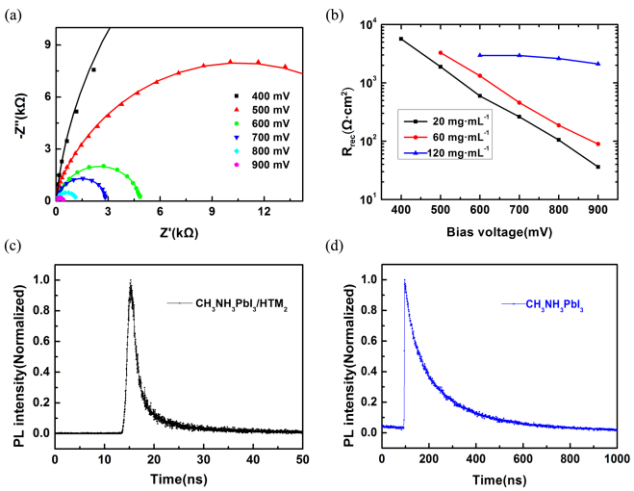

Fig. 3 (a) Nyquist plots of the device with thin layer HTM_2 in the dark over different forward biases, scattered point: experimental data, solid line: fitted curves; (b) Plots of recombination resistance (R_{rec}) *vs* bias voltages for the devices with different thickness HTM_2; (c) and (d) PL intensities for $CH_3NH_3PbI_3/HTM_2$ and $CH_3NH_3PbI_3$

View Article Online
DOI: 10.1039/C4CC02211D
COMMUNICATION

films, respectively, monitored at 775 nm during the transformation. Excitation at 445 nm.

In order to investigate the influence of HTM_2 deposition amount on the cell performance, a series of perovskite solar cells were fabricated by varying spin coating concentration. As shown in Fig. 2(d), with the HTM spin coating concentration increasing, HTM_2 overlayer is getting thicker from unclear to 271 nm, however, the cell performance is getting poorer. At higher concentration, the increasing capping layer thickness will increase the series resistance and cause the *FF* decreased by nearly 50%. The decrease of V_{oc} is mainly due to the dark current augments with the HTM film thickness increasing, lowering the electron concentration as well as their Fermi level.[5] It is thus deduced that, thin HTM layer will facilitate the hole transport as well as the cell performance. Further improvement in the conductivity of the HTM layer as well as the cell performance will be carried out in the future.

To understand the thickness-related influence on the cell performance, electrochemical impedance spectroscopy (EIS) was carried out, in which the potential bias was applied from 400 to 900 mV in the dark in the frequency range from 10^5 to 0.1 Hz (Zahner IM6ex), as shown in Fig. 3(a). According to simplified transmission line model, the main arc is supposed to be the combination of the recombination resistance (R_{rec}) and the chemical capacitance of the film (CPE_{μ}), see Fig. S1.[17,22-23] By fitting the Nyquist plots, the relationship between the R_{rec} and the bias voltage is obtained.[5] From Fig. 3(b), we can see that (1) for the same device, R_{rec} drops with the increasing forward bias voltage, mainly because the Fermi level in the mesoscopic TiO_2 is elevated under the forward bias (> 500 mV) which is beneficial to easy electron flow across $TiO_2/CH_3NH_3PbI_3$ interface; (2) at the same forward bias voltage, with the thickness of HTM increasing, the R_{rec} increases greatly in all bias voltage ranges, indicating thick capping layer is disadvantageous to the charge transfer.[5] Likewise, large R_{rec} will lead to unsatisfactory cell performance, in good agreement with our test result in Fig. 2(d).

Furthermore, time-resolved photoluminescence (PL) decay measurement has been used to research charge transfer at a stable well-defined interface, as shown in Fig. 3(c) and (d). The PL decay time can be obtained after fitting the data with bi-exponential decay function.[24] The $TiO_2/CH_3NH_3PbI_3$ film exhibits a time constant of τ=195.6 ns. Further introduction of the HTM_2 as a quenching layer remarkably facilitates the PL decay with the time constant τ=1.36 ns. This is due to the diffusion of the photogenerated excitons to the $CH_3NH_3PbI_3/HTM_2$ interface where they are quenched. It is thus suggested that the existence of $CH_3NH_3PbI_3/HTM_2$ interface is beneficial to the hole transfer and HTM_2 has excellent hole pumping capacity as well.[25, 26] Finally, the device efficiencies from a batch of ten devices using HTM_2 under the same conditions are given in Fig. S2. We can see that all of them show a PCE over 11% with an average PCE of 11.30%, indicating their good reproducibility. Preliminary stability test has been carried out, that is, unsealed cells were kept in the dark at ambient conditions which were tested every day during 7 days. The cells with HTM_1 and HTM_2 were quite stable, which PCEs are almost constant with 0.2% drop for HTM_1 and 0.9% drop for HTM_2 comparable to their initial PCEs.

Conclusions

In conclusion, we have, for the first time, employed two new triphenylamine-based HTMs containing butadiene derivatives in $CH_3NH_3PbI_3$ perovskite solar cells. Both of them show excellent capacity to hole transport, and up to 11.63% of efficiency has been achieved for the $CH_3NH_3PbI_3$ perovskite solar cell with HTM_2. Their typical advantages are easy synthesis, low cost and relatively good cell performance, which may provide a possibility for commercial application of organolead halide perovskite solar cells in the future.

The authors would like to thank the financial support from the MOST (973 projects, No. 2012CB932903 and 2012CB932904), Beijing Science and Technology Committee (No. Z131100006013003), NSFC (No. 51072221 and 21173260) and the Knowledge Innovation Program of the Chinese Academy of Sciences.

Notes and references

[a] Key Laboratory for Renewable Energy (CAS), Beijing Key Laboratory for New Energy Materials and Devices, Beijing National Laboratory for Condense Matter Physics, Institute of Physics, Chinese Academy of Sciences, Beijing 100190, China. Fax: +86-10-8264-9242; Tel: +86-10-8264-9242; E-mail: qbmeng@iphy.ac.cn, dmli@iphy.ac.cn.

[b] Co-Innovation Center of Chemistry and Chemical Engineering of Tianjin, School of chemical Engineering and Technology, Tianjin University, Tianjin 300072, China. Fax: +86-22-27404208; Tel: +86-22-27892279; E-mail: lixianggao@tju.edu.cn.

† Electronic Supplementary Information (ESI) available: Experimental procedures, fabrication details and device characterization. See DOI: 10.1039/c000000x/

1 A. Kojima, M. Ikegami, K. Teshima and T. Miyasaka, *Chem. Lett.*, 2012, **41**, 397.
2 C. R. Kagan, D. B. Mitzi and C. D. Dimitrakopoulos, *Science*, 1999, **286**, 945.
3 A. Kojima, K. Teshima, Y. Shirai and T. Miyasaka, *J. Am. Chem. Soc.*, 2009, **131**, 6050.
4 J.-H. Im, C.-R. Lee, J.-W. Lee, S.-W. Park and N.-G. Park, *Nanoscale*, 2011, **3**, 4088.
5 H.-S. Kim, C.-R. Lee, J.-H. Im, K.-B. Lee, T. Moehl, A. Marchioro, S.-J. Moon, R. Humphry-Baker, J.-H. Yum, J. E. Moser, M. Grätzel and N.-G. Park, *Sci Rep*, 2012, **2**, 591.
6 J. M. Ball, M. M. Lee, A. Hey and H. J. Snaith, *Energy Environ. Sci.*, 2013, **6**, 1739.
7 J. Shi, J. Dong, S. Lv, Y. Xu, L. Zhu, J. Xiao, X. Xu, H. Wu, D. Li, Y. Luo and Q. Meng, *Appl. Phys. Lett.*, 2014, **104**, 063901.
8 http://www.nrel.gov/ncpv/images/efficiency_chart.jpg.
9 J. H. Heo, S. H. Im, J. H. Noh, T. N. Mandal. C. S. Lim, J. A. Chang, Y. H. Lee, H. J. Kim, A. Sarkar, M. K. Nazeeruddin, M. Grätzel and S. I. Seok, *Nat. Photonics*, 2013, **7**, 486.
10 F. D. Giacomo, S. Razza, F. Matteocci, A. D'Epifanio, S. Licoccia, T. M. Brown and A. D. Carlo, *J. Power Sources*, 2014, **251**, 152.
11 B. Cai, Y. Xing, Z. Yang, W.-H. Zhang and J. S. Qiu, *Energy Environ. Sci.*, 2013, **6**, 1480.
12 D. Q. Bi, L. Yang, G. Boschloo, A. Hagfeldt and E. M. J. Johansson, *J. Phys. Chem. Lett.*, 2013, **4**, 1532.
13 J. Burschka, N. Pellet, S.-J. Moon, R. Humphry-Baker, P. Gao, M. K. Nazeeruddin and M. Grätzel, *Nature*, 2013, **499**, 316.
14 M. Liu, M. B. Johnston and H. J. Snaith, *Nature*, 2013, **501**, 395.
15 D. Liu and T. L. Kelly, *Nat. Photonics*, 2014, **8**, 133.
16 N. J. Jeon, J. Lee, J. H. Noh, M. K. Nazeeruddin, M. Grätzel and S. I. Seok, *J. Am. Chem. Soc.*, 2013, **135**, 19087.
17 J. A. Christians, R. C. M. Fung and P. V. Kamat, *J. Am. Chem. Soc.*, 2014, **136**, 758.

18 L. Y. Han, Master Thesis, Tianjin University, 2013.
19 J. H. Noh, S. H. Im, J. H. Heo, T. N. Mandal and S. I. Seok, *Nano Lett.*, 2013, **13**, 1764.
20 X.-Z. Guo, Y.-H. Luo, Y.-D. Zhang, X.-C. Huang, D.-M. Li and Q.-B. Meng, *Rev. Sci. Instrum.*, 2010, **81**, 103106.
21 L. J. A. Koster, V. D. Mihailetchi, H. Xie and P. W. M. Blom, *Appl. Phys. Lett.*, 2005, **87**, 203502.
22. H.-S. Kim, J.-W. Lee, N. Yantara, P. P. Boix, S. A. Kulkarni, S. Mhaisalkar, M. Grätzel and N.-G. Park, *Nano Lett.*, 2013, **13**, 2412.
23 H.-S. Kim, I. Mora-Seró, V. Gonzalez-Pedro, F. Fabregat-Santiago, E. J. Juarez-Perez, N.-G. Park and J. Bisquert, *Nat. Commun.*, 2013, **4**, 2242.
24 J. You, Z. Hong, Y. Yang, Q. Chen, M. Cai, T.-B. Song, C.-C. Chen, S. Lu, Y. Liu, H. Zhou and Y. Yang, *ACS nano*, 2014, **8**, 1674.
25 S. D. Stranks, G. E. Eperon, G. Grancini, C. Menelaou, M. J. P. Alcocer, T. Leijtens, L. M. Herz, A. Petrozza and H. J. Snaith, *Science*, 2013, **342**, 341.
26 P. E. Shaw, A. Ruseckas and I. D. W. Samuel, *Adv. Mater.*, 2008, **20**, 3516.